

THE APPLICATION OF GRIDREFINEMENT, GRIDGATHERING AND MOVING GRID IN EOR SIMULATION

Z.E. Heinemann* and C. Brand*

تطبيقات تحسين وتجميع وتغيير التقاسيم المكانية في محاكاة الإسترداد الإضافي

ز. هينمان وك. براند

يصل طول ضلع شبكة التقسيم في نظام محاكاة النفط الثقيل إلى 100 م في المكمن ذات طاقة الدفع المستنفذة ، الذاتية . كما أن طرق الإسترداد الإضافي مثل الإزاحة المتجانسة والإزاحة البخارية والغمير الكيميائي والإحراق الداخلي تتطلب تقسيم المكمن إلى مساحات صغيرة بطول ضلع يتراوح ما بين 0.5 إلى 10 أمتار. غير أن هذه التقسيمات تعتبر مستحيلة فنياً وعملياً عند تطبيقها في محاكاة المكمن النفطية . تشير هذه الدراسة ، التي تعتمد على طريقة التحكم في الحجم التفردى للمكمن ، على أن تحسين شبكة تقسيم محاكاة المكمن هي إمتداد للطرق المتبعة عملياً في محاكاة المكمن النفطية . وحيث أن التقاسيم الصغيرة للمكمن النفطي مطلوبة فقط عند مقدمة سواحل المكمن المزاحة ، لذلك فأن تحسين حجم المكمن مطلوبة فقط في هذه المنطقة .

ABSTRACT

In black oil simulation, the areal block size can have a magnitude of 100 m by water drive and can extend to 1000 m by depletion drive. EOR displacement processes such as miscible and steam drive, surfactant flooding and in situ combustion require 10 to 0.5 m grid spacing. This is technically impossible in field scale simulation which uses a conventional Cartesian grid.

This paper, based on the control volume discretization technique, shows that local grid refinement is a straightforward extension of industry standard methods. Applying some simple rules, the locally refined grid is strictly orthogonal, even at the fine-coarse grid transition. This orthogonality is a fundamental requirement to make sure that the numerical solution converges to the true one if the grid size is reduced.

Since small block size is only required at the displacing front, local grid refinement is applied only in this area and moves forward in time. With dynamic grid refinement, the down-streams block ahead of the front are subdivided before the displacing front arrives and

they are gathered again when the front has passed them. By gathering the blocks outside the EOR area, the overall block number can be reduced considerably without neglecting the influences of the environment.

An example for miscible hydrocarbon gas drive illustrates the combination of dynamic grid refinement and gathering, showing that a field scale EOR displacement can be simulated with small block size without exceeding the technical and economic limits.

INTRODUCTION

Numerical simulation has become one of the most important tools to solve complex reservoir engineering problems. Based on a mathematical description of the physical system, a set of non linear differential equations are solved numerically and the result is compared with the observations. By tuning reservoir parameters, called history matching, a numerical reservoir model is created which is able to reproduce the real reservoir performances and gives the possibility of predicting future behaviour. A good fitting neither confirms the mathematical description nor proves the accuracy of the numerical

*HOT Engineering Ges.m.b.H., Austria

solution or genuine reservoir data. Inaccuracies on one side are counterbalanced by deviations on other side. This circumstance does not restrict the applicability of the model provided that no greater change in the reservoir mechanism takes place.

In black oil simulation, the mathematical description is simple and well defined. The result is not seriously influenced by the numerical solution techniques in use. The number of system variables is limited and identical in time and space. However, it is important that enough observations are available to confirm the reliability of the numerical reservoir model.

When dealing with enhanced recovery processes, the situation is rather different. A large variety of methods exists and the possibilities in mathematical description are wide spread. The physical and chemical natures of the ongoing processes change dramatically in time and space, differing fundamentally from the primary ones. The history matching based on black oil type simulation gives no or very limited guarantee for realibility of the EOR prediction. In most of the cases is it inaccurate to speak about simulation, because no possibility is given to compare the model with observations of the real reservoir. What normally is done is simply mathematical-numerical modelling the reliability of which can only be based on the complete and correct mathematical formulation, on the accurate numerical solution and the complete and proper accounting of the influence of reservoir properties.

This paper focuses on gridding to show the necessity and practical applicability of grid refinement and gathering. Local grid refinement is necessary to get enough small blocks at the area of interest and gathering makes it possible to consider the environment without spending computer time and money to calculate unnecessary details. The possibility to change the grid over time, by the user or automatically, increases the flexibility of these techniques considerably. The methods are applicable for modelling of miscible drive, polymer and surfactant flooding, steam drive and in situ combustion and also for conventional black oil and compositional simulation.

FINITE CONTROL VOLUME FORMULATION OF THE FLOW EQUATION

The reservoir system is formed by the formation rock given the frame for the pore space and K chemical components. The pore space is filled out by P phases, may be vapor, liquid or solid. Each fluid phase contains up to K chemical components.

The first and most fundamental step in the development of any reservoir simulator is the description of the physical phenomena by a set of equations. This

equation system contains mole (or mass) balances for each component and one energy balance equation. Additional information, in the form of constitutive equations is needed to define the intrinsic response of the material in question. They formulate the relations between driving forces and transport velocities and the mathematical properties (as densities and viscosities) to the state variables. In reservoir simulation, conditions of thermodynamic equilibrium are commonly assumed. The assumption of equilibrium, while questionable in many situations, plays an important role in the derivation of the final form of the mathematical model.

The equation system in question is very complex and non linear. Analytical solution is possible only after strong simplifications, thereby losing the applicability to real reservoir problems. Though a number of numerical techniques have been tried, almost all such problems are solved through the finite difference method. For this reason, the discussion in this paper is limited to this method.

The finite difference method, especially in the form of the finite volume technique, has some theoretical and numerical advantages. The difference equations can be easily identified with the corresponding differential equations and the solution of the finite difference equations is more straightforward. Most importantly it is possible to identify the numerical terms with the reservoir ones. The control volume represents a defined part of the reservoir and all properties and variables assigned to the grid point are averages for this volume.

Before going on to solve the equation system, certain substitutions are made to reduce the number of unknowns and equations per grid point. The phase pressures, except one, are eliminated through the capillary pressure equations, a part of the mole fractions are eliminated using mole constraints and phase equilibrium conditions. Darcy's law is substituted to eliminate phase velocities as variables. The variables eliminated by substitution are called secondary. They do not eliminate primary variables. Some of the primary variables existing only in equations belonging to one grid point can be eliminated by partial elimination. The variables solved simultaneously for all grid points are the implicit variables. The eliminated the explicit ones.

With growing complexity of the mathematical description, increases the variety for selection of primary-secondary and implicit-explicite variables and the resulting equations bring advantages and disadvantages by the numerical solution (more or less stability, higher or lower convergence rate by the Newton iteration, etc.). One of the advantages of the finite difference method is that substitution and partial elimination can be done before and after discretisation. It is possible to do it algebraically or

numerically assuring great flexibility, especially important when dealing with EOR models. The wide range of EOR technologies and possible description of the physical phenomenon requires such a flexibility.

An integral approach similar to the one described by Nghiem [1], and Pedrosa and Aziz [2] is applied to derive the multiphase flow equations.

The conservation of mass for the component k :

$$-\iint_{A_I} \left[\sum_{p=1}^P \bar{u}_p \xi_p x_{pk} M_k \right] \bar{n} dA + \iiint_V q_k M_k dV = \frac{\partial}{\partial t} \iiint_V \left[\phi \sum_{p=1}^P S_p \xi_p x_{pk} M_k \right] dV. \quad (1)$$

V is a finite control volume around the grid point I (Fig. 1). The first term on the left-hand side is the *convection term*. Its physical meaning is very easy to understand. \bar{u}_p is the phase velocity with dimension $m/s = m^3/(s \ m^2)$ and gives the phase volume flowing per second through a unit surface perpendicular to the flow direction. ξ_p is the mole density *mole/m³* of the phase, and the product $\bar{u}_p \xi_p$ is the mole velocity in *mole/(s m²)*. This is the number of moles flowing through the unit surface. Multiplying by the mole fracture x_{pk} and the mole weight M_k *kg/mole* one gets the mass velocity *kg/(s m²)* of component k . On the surface of the control volume, the mass velocity can be split into two components: one parallel to the surface, the other orthogonal on it. We obtain the orthogonal component by multiplying the velocity with the normal unit vector \bar{n} . The expression

$$\sum_{p=1}^P [\bar{u}_p \xi_p x_{pk} M_k] \bar{n} dA \quad (2)$$

is the mass flow rate *kg/s* of component k through the elementary surface dA . The summation over all phases is necessary, because the given component can be present in, and transported by, several phases. The integral over the closed surface A_I is the total mass flow rate of component k , flowing in or out from the control volume. Because the normal vector is oriented outwards, the integral is positive if more mass is flowing out than flowing in.

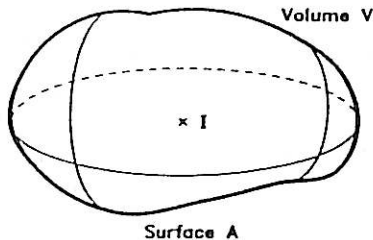


FIG. 1. Control volume around the grid point.

The second term is the *source* (or sink) rate. It determines how much mass of component k directly will be taken out of, or supplied into, the control volume per time unit. In the case of a point source, interpreted as a well within the volume, the volume integral can be replaced by the value Q_{kI} . The left-hand side of Eq. 1 is also the mass exchange rate between the control volume and the outside world. The right-hand side of Eq. 1 is the *accumulation* term. The volume of phase p per unit rock volume is $\phi S_p m^3$. It contains $\phi S_p \xi_p$ moles and $\phi S_p \xi_p x_{pk} M_k$ mass *kg* of the component k . The summation over all phases and the integral over the whole control volume gives the mass of component k within the control volume. The derivative with respect to time is the mass accumulation rate for component k in the control volume.

Eq. 1 is a mole balance. As a matter of fact, mass and mole balances are equivalent. This will be evident by cancelling the constant mole mass M_k from both sides of Eq. 1. In petroleum engineering, standard volumes are often used to express material quantities. Let ρ_k^0 be the standard density of the pure component k (which is a constant). Dividing both sides of Eq. 1 by ρ_k^0 , it becomes a volume balance. Such a formulation is commonly used in the so called *black oil models* with three components: oil, gas and water. It is easy to show that the integral form of the flow equation is equivalent to the commonly used differential form. The permeability of the porous medium is defined *via* the Darcy law, which we write immediately for a multiphase case:

$$\bar{u}_p = -\frac{k_{rp}}{\mu_p} \bar{k} \nabla \Phi_p = -\lambda_p \bar{k} \nabla \Phi_p, \quad (3)$$

$$\nabla \Phi_p = \nabla p_p - \rho_p \bar{g}. \quad (4)$$

In general, the permeability \bar{k} is a symmetrical tensor:

$$\bar{k} = \begin{bmatrix} k_{11} & k_{12} & k_{13} \\ k_{21} & k_{22} & k_{23} \\ k_{31} & k_{32} & k_{33} \end{bmatrix}, \quad (5)$$

where $k_{ij} = k_{ji}$.

Substituting the flow term of Eq. 1 for velocity according to Eq. 3, and splitting up the integral into a sum over all the surfaces connecting block I with its neighbours $J = 1, \dots, NJ$, one obtains

$$\begin{aligned} & \iint_{A_I} \sum_{p=1}^P \xi_p x_{pk} \lambda_p (\bar{k} \nabla \Phi_p) \cdot \bar{n} dA \\ &= \sum_{J=1}^{NJ} \iint_{A_{IJ}} \sum_{p=1}^P \xi_p x_{pk} \lambda_p \nabla \Phi_p (\bar{k} \bar{n}) dA \\ &= \sum_{J=1}^{NJ} Q_{IJk}, \end{aligned} \quad (6)$$

where Q_{Ijk} , the flow of component k from I to J , is

$$Q_{Ijk} = - \iint_{A_{IJ}} \sum_{p=1}^P \Lambda_{pk} \nabla \Phi_p(\bar{k}\bar{n}) dA \quad (7)$$

$$\Lambda_{pk} = \xi_p x_{pk} \lambda_p \quad (8)$$

The sequence of multiplications in the term $\bar{k}\nabla\Phi_p\bar{n}$ can be changed, because \bar{k} is a symmetrical tensor. Eq. 1 can be written in the following form:

$$\sum_{j=1}^{NJ} Q_{Ijk} + \iiint_{V_I} q_k dV = \iiint_{V_I} \frac{\partial}{\partial t} \left[\phi \sum_{p=1}^P S_p \xi_p x_{pk} \right] dV \quad (9)$$

Discretization

Looking for approximative values of the solution only on a set of grid points and only for discrete time-levels, the differential equations are reduced to a finite-dimensional system of algebraic equations. The process is called discretization. It involves the construction of an appropriate grid system and the set up of proper equations, one or more per grid point.

Consider the grid block shown in Fig. 2. The volume of the block is V_I , x_I is the gridpoint in the centre of the block, and x_J is the grid point in the J -th neighbour block. A_{IJ} denotes the communication surface between blocks I and J . In the general case, the block is confined by curved surfaces which can be approximated by planes.

For the flow terms (Eq. 7)

$$Q_{Ijk} = \iint_{A_{IJ}} \sum_{p=1}^P \Lambda_{pk} \nabla \Phi_p(\bar{k}\bar{n}) dA \quad (10)$$

- the surface A_{IJ} connecting the block I with its J -th neighbour
 - the scalar product $\nabla\Phi_p(\bar{k}\bar{n})$
 - the component mobility Λ_{pk}
- have to be approximated.

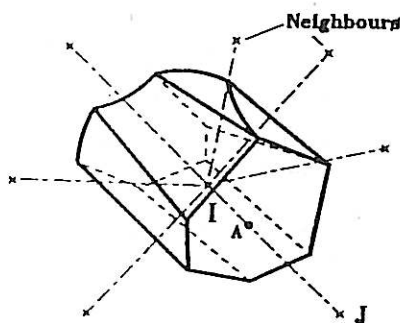


FIG. 2. A grid block.

The surfaces A_{IJ} and the orientation of the unit normal vectors \bar{n}_{IJ} are determined by the rules of grid construction. Once the grid is given, area and orientation can be computed exactly by means of geometry.

For the approximation of the scalar product $\nabla\Phi_p(\bar{k}\bar{n})$, an isotropic porous medium has to consider at first. In this case, the tensor can be replaced by a scalar value k .

In the general case, all grid points forming tetrahedrons with intersection with the individual block surface have to be taken into consideration (Fig. 3). However, the scalar product $\nabla\Phi \cdot \bar{n}$ can be approximated by a more simple formula if the vector \bar{n} is parallel to the vector h_{IJ} , i.e. the surface connecting blocks I and J is orthogonal to the straight line connecting the grid points I and J . Therefore,

$$\nabla\Phi \cdot \bar{n} = \frac{\Phi_J - \Phi_I}{h_{IJ}} \quad (11)$$

For the orthogonal case, flow terms are therefore given by

$$Q_{Ijk} = \tau_{IJ} \sum_{p=1}^P (\Lambda_{pk})_{IJ}^{n+1} (\Phi_J - \Phi_I)_p^{n+1} \quad (12)$$

where

$$\tau_{IJ} = \frac{A_{IJ}}{h_{IJ}} k_{IJ} \quad (13)$$

is the interblock transmissibility. Eq. 13 is often used if the block surface is non orthogonal to the connection line h_{KJ} . This is erroneous, because the calculated flow rate does not converge to the true value if $h_{IJ} \rightarrow 0$. That means the approximation is not consistent. In the following, grid refinement will be proposed as a possibility to improve the accuracy, but this only makes sense if the grid is orthogonal.

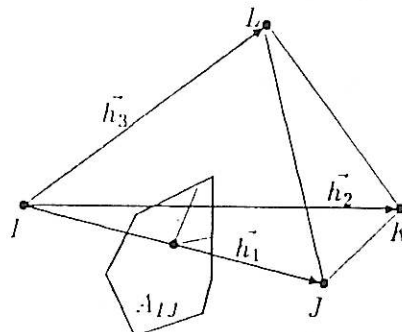


FIG. 3. Grid element and communication surface between blocks I and J .

In cases where a scalar permeability cannot model the flow behaviour in a porous medium, a tensor \bar{k} is introduced. The Darcy law, Eq. 3, establishes a linear relationship between the potential gradient $\nabla\Phi$ and the flow velocity \bar{u} . In general, this linear dependence alters the absolute value of $\nabla\Phi$ and its direction. Flow velocity is no longer parallel to the potential gradient.

By using *finite volume techniques* the flow term $\nabla\Phi_p(\bar{k}\bar{n})$ can be calculated in the same manner as for the isotropic case. The only difference is that $\nabla\Phi_p$ is multiplied with the vector $\bar{k}\bar{n}$ instead of $k\bar{n}$. Or for general grids, the grid-block must be constructed so that the communication surfaces are \bar{k} -orthogonal (orthogonal in a general sense, defined by $\bar{k}\bar{n}$ parallel to \bar{h}) on the straight lines connecting adjacent blocks. In analogy to the derivation of Eq. 12,

$$\nabla\Phi \cdot (\bar{k}\bar{n}) = |\bar{k}\bar{n}| \frac{\Phi_J - \Phi_I}{h_{IJ}} \quad (14)$$

Fig. 4 shows how an orthogonal Cartesian block system is altered by the concept of \bar{k} -orthogonality. In this example,

$$\bar{k} = \begin{pmatrix} 3 & 1 \\ 1 & 3 \end{pmatrix}, \quad (15)$$

the principal axes are oriented diagonally. Note that for this reason, the surfaces connecting the block to its diagonal neighbours are orthogonal (in the usual sense) to the connecting line.

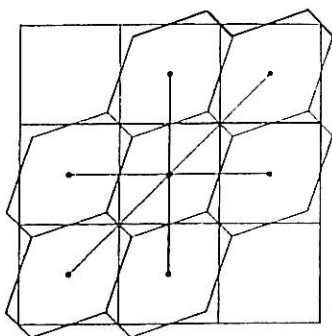


FIG. 4. \bar{k} -orthogonal block system.

The Component Mobility

Since Q_{IJk} given by Eq. 7 is a surface integral, the component mobility Λ_{pk} is required on A_{IJ} , which lies somewhere between grid points I and J . However, the state variables are assigned to the grid points. To get approximate values for Λ_{pk} , some sort of averaging between the values at points I and J is necessary. It can be demonstrated that midpoint weighting has lower truncation error, but both Peaceman [3] and Russel and Wheeler [4] point out that midpoint

weighting may lead to oscillations and overshoot in the solution upstream of the front. The easiest is to take the value for the upstream grid point, leading to the industry standard up-stream weighting. The up-stream weighting is stable when variables are taken at the current time level (implicit mobility) and conditionally stable when calculated at the old time level (explicit mobility). However, upstream weighting does have a serious price related to its higher truncation error, smearing out the sharpness of the front. Ewing [5] discusses some of the disastrous effects of up-stream weighting. Many proposals have been made to reduce this numerical dispersion, including the use of dynamic weighting, but only one possibility is practical namely reducing the distance between the grid points and increasing the number of blocks between injection and production wells.

Perry and Herron [6] and Snyder [7] showed that by immiscible gas displacement under practical conditions, the saturation distribution is wrong for 3 blocks on the head of the displacement front (Fig. 5). This smearing out effect leads to early breakthrough and overestimate of the overall GOR, but has no significant effect on the cumulative oil production. With most EOR displacement, the composition through determination of the existing phases and their properties as viscosity, interfacial tension etc., plays a decisive role. The numerical dispersion smears out not only the saturation profile, but also the composition one. As a consequence, in a given point (or block) between the injection and production wells, the concentration required for miscibility will be achieved later in a numerical simulation as in reality.

A good example for this error was published by Coats [8]. The length of the linear model reservoir was 60 m. The reservoir oil composed of methane, butane and decane (20/20/60 mole %) was displaced by a methane and butane mixture (68.4/31.6 mole %). The numerical simulation was performed using 80, 40 and 20 grid blocks. The block lengths were 1, 2 and 4 m.

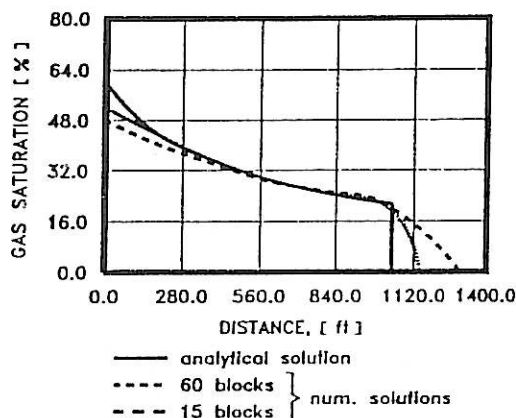


FIG. 5. Numerical solution of a linear gas displacement with different block sizes [7].

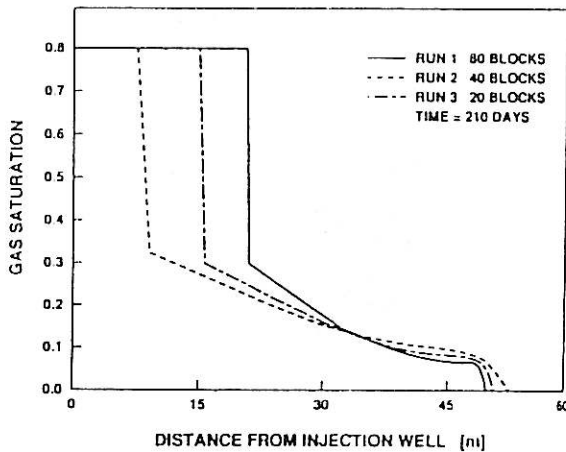


FIG. 6. Calculated gas saturation vs. distance for multi-contact miscible gas drive [8].

Fig. 6 shows the calculated gas saturation profiles vs. distance at 210 days. The discontinuities show the position of the miscible front. It is clear, that a correct calculation of the displacement process requires a block width in magnitude of 1m.

Similar results were published by Nghiem and Li [9]. In a low temperature CO₂ flooding, 0.3 m block size gives satisfactory matching for slim-tube displacement. The reduction of size to 0.15 m showed no significant changes.

Accumulation Term

In the accumulation term of Eq. 1,

$$\iiint_{V_I} \frac{\partial}{\partial t} \left[\phi \sum_{p=1}^P S_p \xi_p x_{pk} \right] dV, \tag{16}$$

we replace the time derivative by a difference approximation. The volume integral is evaluated approximately as the value of the integrand at point *I*, times the block volume. This results in

$$\left(\iiint_{V_I} \frac{\partial}{\partial t} \left[\phi \sum_{p=1}^P S_p \xi_p x_{pk} \right] dV \right)^{n+1} \approx \frac{V_I}{\Delta t} \left(\left[\phi \sum_{p=1}^P S_p \xi_p x_{pk} \right]_I^{n+1} - \left[\phi \sum_{p=1}^P S_p \xi_p x_{pk} \right]_I^n \right) \tag{17}$$

where *V_I* denotes the volume of gridblock *I*, *n* is the index for the time level, *tⁿ⁺¹* = *tⁿ* + Δ*t*. In the discretization for this term and also for the source term, an irregular shape of the gridblock has no influence as long as the block volume is evaluated correctly.

The accumulation term for the energy balance equation has a similar form. By simulation of in situ combustion this term plays a critical role. The high temperature burning zone has an extension of 0.3 to 1 m. If the block size is larger than this, the average

temperature of the block will be lower than the reaction temperature. Consequently, the burning front extinguishes. Chu [10] showed that the grid block size would have to be in the order of half-a-meter.

BLOCK SIZE IN NUMERICAL SIMULATION OF EOR PROCESSES

In black oil simulation, the areal block size can be in the magnitude of 100 m by water drive and can be extended to 1000 m by depletion drive. That means 2000–10,000 blocks per layer in the case of an average oil reservoir. Taking 3–10 layers vertically means 6000–100,000 blocks in a conventional Cartesian grid. The upper limit is nowadays the maximum which can be handled with the largest and fastest computers.

Reducing the block size to 10 m, the number of blocks explodes to 0.5 to 10 million and 10 m is still to large for some important EOR displacement processes. This is the reason that most of simulation studies were limited to symmetry elements of pilot areas.

Theoretically there are two possibilities to overcome this difficulty:

- local grid refinement, and
- front trucking.

Local grid refinement is an extension of the generally used finite difference technique. In front trucking, the steady-state pressure distribution is calculated for fixed saturation and composition distribution. This determines the velocity of the displacing fronts and it is possible, taken into consideration the overall material balances, to determine their new position a time step later. Recent publications [11] presented results for two phase immiscible displacement. Future investigations have to show the applicability for more realistic cases. In this paper, only local grid refinement will be discussed, already applied in commercial simulators.

Local Grid Refinement

A simple Cartesian grid, also when using variable grid spacing, is frequently not sufficient for supplying a good description of particularly interesting areas, e.g. in the vicinity of the displacing front.

In order to achieve a high resolution by means of as few blocks as possible, selected area or individual blocks can be subdivided by means grid refinement. This method was used for reservoir simulation by Von Rosenberg [12] and Heinemann *et al.* [13–15] at first.

The initial block system is called fundamental and its blocks are referred to as fundamental blocks (Abbreviate: *F*-blocks). They are defined by three indices *I1*, *I2*, *I3* for the 3D-space. Three divisor numbers (*KI1*, *KI2*, *KI3*) are assigned to every *F*-block. They indicate the number of partial blocks into which the *F*-block is to be subdivided in the corresponding direction. In this

way, sub-coordinates ($I1T$, $I2T$, $I3T$) are defined in every F -block, having the same direction as the main coordinates (Fig. 7).

In this way each partial block can be addressed by specifying the coordinates ($I1$, $I2$, $I3$). Partial blocks are referred to as R -blocks (refinement) in the following.

For a correct calculation of the transmissibility it is necessary to modify the block boundaries on the transition surface of the coarse and refined grid. Fig. 8 shows a correct refinement.

The communication surface between F - and R -blocks is orthogonal on the grid line \overline{IJ} and so, as shown previously the difference approximation will be consistent.

It is easy to understand that this solution has some limitations. It is applicable only if the refinement is 1:2 (Fig. 9) for each direction. The second problem is if there is a refinement on both sides of a grid block, one gets complications in the calculation of the transmissibilities. For blocks with stretched shape it is not possible to construct such a geometry. The last problem rises when regarding the vertical directions. In consequence the following rules have to be considered for subdivision of fundamental blocks:

1. If the neighbouring F -blocks of an F -block in one coordinate direction are looked at, the divisors for the two other coordinate directions are not allowed to increase for both of the neighbouring F -blocks.

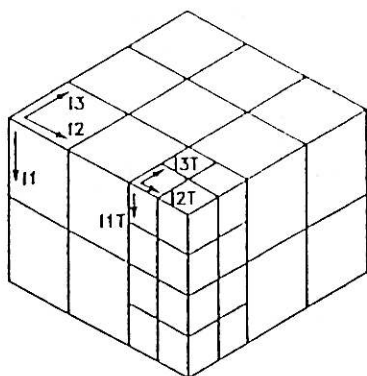


FIG. 7. Determination of subcoordinates.

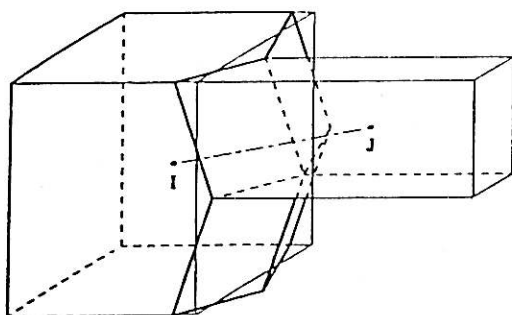


FIG. 8. Distortion of block interfaces in a three-dimensional grid. The fundamental block (left) has a neighbouring block divided into four subblocks.

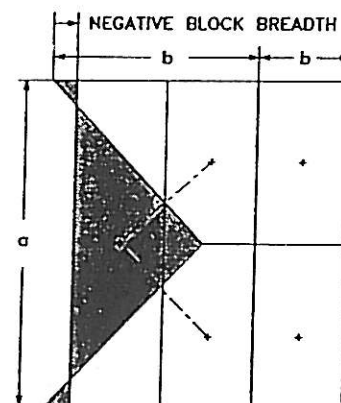


FIG. 9. No orthogonal refinement possible by stretched blocks.

2. At any section through the block system, one block may only have one or two neighbouring blocks on each side.
3. The division in the vertical direction must be continuous within communicating layers, *i.e.* the divisor for the directions $I2$ and $I3$ are the same for neighbouring F -blocks lying one below the other.
4. If two F -blocks in one coordinate direction are looked at, it is not allowed that one of the divisors of the two other coordinate directions increases and the other decreases.

In a conventional Cartesian block system using a five-point differential scheme, a block has a maximum of four neighbours in the two-dimensional case, and a maximum of six neighbours in the three-dimensional case.

For a local grid refinement, a block can have a maximum of twelve neighbours, taking into consideration rules 1-4.

True and Patch Refinement

Two different type of local grid refinements have been applied in reservoir simulation:

- True refinement
- Patch refinement

The first technique is a true local grid refinement where an arbitrary level of refinement can be applied at any region or point of space. With true refinement, all grid points are integrated into the same equation system. A conventional Cartesian grid with natural ordering (follow the coordinate axis) leads to a linear algebraic equation system with regular band matrix with uniform bandwidth. The solution algorithm for these types of equations is well known and a good vectorisable. Local grid refinement disturbs this regularity and needs special matrix solvers. They cannot be so fast because the position of the non zero coefficients are not known a priori. This type of refinement cannot be adapted to conventional

simulators because a different algorithm and code structure are required. It was mentioned [16], that the overhead associated with the data structures and the grid generation can dominate the overall computation time. This statement does not fit with the experiences of the author. Developing new matrix solvers, special for irregular linear equation systems, can reduce the overhead considerably [17].

The performances are the same as for the conventional block model with the same grid size. Experiences have shown that the true refinement is general applicable and has no limitation in respect to flow direction, saturation, distribution etc. In this paper all discussion are related to truly refinement.

By patch refinement the equations are solved on the coarse grid at first. This coarse grid overlap the refined area. Afterwards, some of the grid points serve as boundary points to solve a second system of equations for the refining grid points. The advantage of this type of refinement is that the matrix remains regular and can be solved faster. The decoupling of the refined part of the grid leads to serious instabilities and cannot be used if the flow is directed from the refined grid towards the coarse one. In this case the upstream block is refined and has different saturations and overall composition as the corresponding coarse block. If any, then the patch refinement can be used but only if the transition surface between the coarse and fine grid is far enough from the place of interest.

Gathering

Applying grid refinement one can get a higher resolution in the vicinity of the wells, boundaries and discontinuities. Practical applications have shown that the reverse procedure, *i.e.* constructing a block system by block gathering, may be very useful. This technique was introduced by Heinemann and Munka [18].

Fig. 10 shows one part of a fundamental Cartesian grid. Once 8 blocks and twice 2 blocks were gathered. The same block system can be constructed through refinement. In Fig. 10 one block was sub-

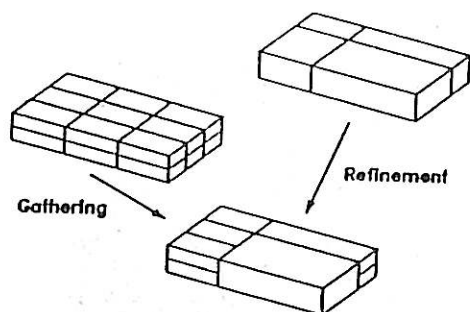


FIG. 10. Construction of a block system by block gathering and refinement.

divided 4 times and two blocks twice. A gathered block system is consistent under the same conditions as the refined block system. The rules of that are given in the previous section.

Primary and Secondary Grid

The reservoir is known through the structure map, gross and net thickness, porosity distributions *etc.* We apply a block system which approximates more or less the geometry. We assign parameters to the blocks which are average values for that part of reservoir represented through the block volume. The average pressure and saturations will be calculated for each block under consideration of the phase contact, the *PVT* and rock properties. In this way the block system is initialized. The average reservoir pressure and the petroleum in place can be compared with the forgoing volumetric reserve estimation. If the initialization is right, the model will be in hydrodynamic equilibrium. The grid model is called *primary grid*.

We can change the block system through subdivision of the blocks or through gathering. The combination of these, that means construction of new blocks from subdivided ones, can be used, even when it is a little bit complicated. Such a rebuilding of the block system has to conserve the mass. That means no change in the amount of fluid in place is allowed. The parameters of the blocks have to be calculated from the previous block system and not from the maps. The new system is called *secondary block system*.

Our expectation is that if the primary grid was in a hydrodynamical equilibrium the secondary has to be near this stage.

Dynamic Grid Refinement

Refinement and gathering can be done in every stage of the simulation run. The only problem is to assign the right pressure, saturations and compositions to the new blocks. Fig. 11 shows a linear

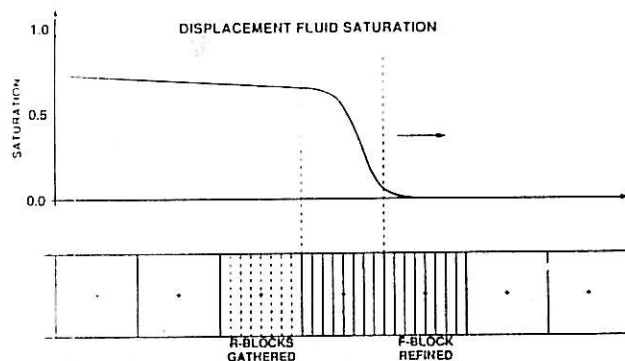


FIG. 11. Linear displacement with dynamic grid refinement.

displacement with pressure and saturation distribution. Ahead of the displacement front the saturation is homogeneous. If the coarse grid is refined here before the displacement front arrives, the same saturation to all refined block, equal to can be assigned themselves of the coarse grid. The pressure is not critical because it is calculated implicitly in the next time step and the assigned values have no influence on that.

Behind the front saturation (and composition) gradient is moderate. Blocks can be gathered and the volume average values can be assigned to the new ones. The automatic and continuous application of this procedure leads to the moving grid. The grid is refined only on the displacing front and moves with it.

The refinement and gathering of the blocks is regulated by two sets of parameters:

- Maximal pressure, saturation and concentration gradients before a fundamental block
- Maximal pressure, saturation and concentration between refined blocks within a fundamental block.

After every time step it will be shown if at least one of the gradients is higher than the limit. If this is the case, the downstream block will be refined for the according coordinate direction. Afterwards, it will be proved if the rules of refinement are satisfied or not and supplementary refinement done if necessary in the surrounding blocks. It is assured that the displacement front is always placed in the refined area. The second condition will be proved only in given time points to avoid a continuous jump between refinement and gathering.

Dynamic grid refinement brings a certain overhead in the numerical calculation, but this is not very much. This will be demonstrated by a simple example which is well documented by Odeh [19]. Areal and cross-section views of the reservoir are given in Fig. 12. The reservoir is initially undersaturated. A gas injection well is located at the grid point (1,1,1) and a producing well at (3,10,10). Pertinent data, PVT properties and relative permeabilities can be taken from the original Odeh paper.

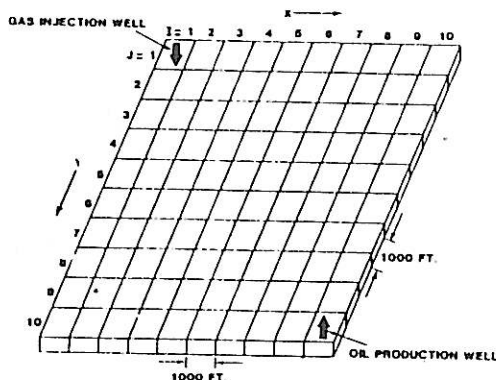


FIG. 12. SPE First Comparative Solution Project. Grid system and diagonal cross section [19].

A $3 \times 5 \times 5$ grid was taken with 2×2 refined blocks at the well location. The number of blocks are 93 compared with the 300 blocks in the original $3 \times 10 \times 10$ grid. The same data and constraints were used as in the original example (Case A).

For every block a 2×2 horizontal dynamic refinement was allowed. A block would be refined if the difference between two neighbouring blocks exceeds in saturation 0.05 or in pressure 20 bars. For case B the block gathering, that means the reconstruction of the original blocks, was not allowed. In case C this happens if the maximal saturation and pressure differences between the refined blocks within a fundamental one become less than 0.05 and 10 bars.

Fig. 13 shows number of blocks vs. production time. Fig. 14 gives the block systems of cases B and C at gas breakthrough. The results were in every respect practically identical and as good as for the basic case. Fig. 15 compares the CPU-times and gives an impression of the advantages of dynamic grid refinement.

To evaluate the computational efficiency of local refinement the 10 years producing period with time step 90 days is simulated. The simulation was run on the DEC Microvax-II computer. For both cases the finite difference equations are solved respectively by IMPES, semiimplicit, and fully implicit (Newton-Raphson Iteration) solution methods. The matrix is solved by an iterative solver. The production results

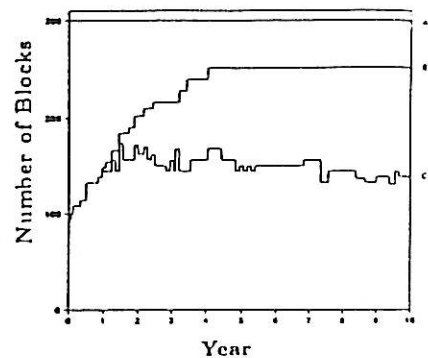


FIG. 13. SPE First Comparative Solution Project. Number of blocks vs. production time.

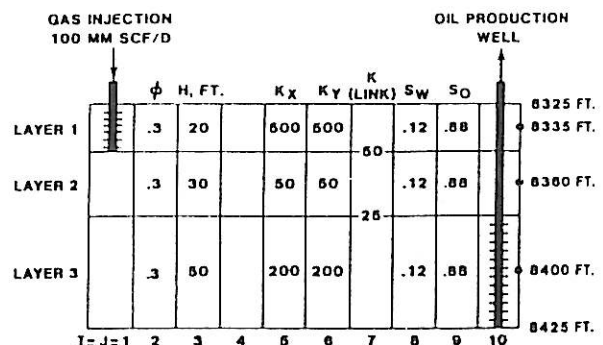


FIG. 12. SPE First Comparative Solution Project. Grid system and diagonal cross section [19].

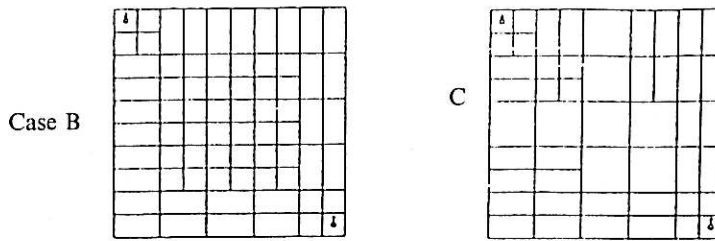


FIG. 14. SPE First Comparative Solution Project. The blocksystem at gas breakthrough for cases B and C.

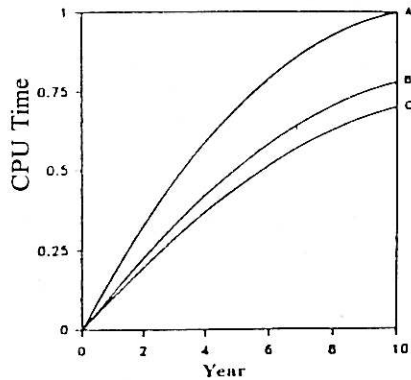


FIG. 15. SPE First Comparative Solution Project. Comparison the CPU time for dynamic refinement.

in both cases were in good agreement for all three solution methods.

The CPU time per matrix-solution and per variable of case B is larger than that of case A. This is caused by the irregular matrix structure of case B, but is compensated by the reduction of block number. In the average, 23% reduction of block number could save 10% of CPU time.

EXAMPLE

To transmit the idea of combined application of dynamic grid refinement and gathering by EOR simulation studies, an example will be presented.

The fundamental block system has an extension of $5 \times 30 \times 40 = 6000$ blocks. The block size in the productive area is 100×100 m. Rich HC gas is injected on the top of the relatively flat anticlinal in one well with $300,000 \text{ sm}^3/d$ rate. The area of interest was refined 2×2 to get 50×50 m block size and outside the blocks are gathered to save CPU-time. The block model is shown in Fig. 16. Note that in the area which will not be touched by miscible drive, the blocks are gathered vertically as well, leading to a two dimensional model for this part of the reservoir. The surrounding of the EOR area is described just coarsely, but still the whole hydrodynamic unit is included in the calculations. This refined/gathered model has 3660 blocks. The conventional model with the same block size in the central area, shown in Fig. 17, would have 8640 blocks.

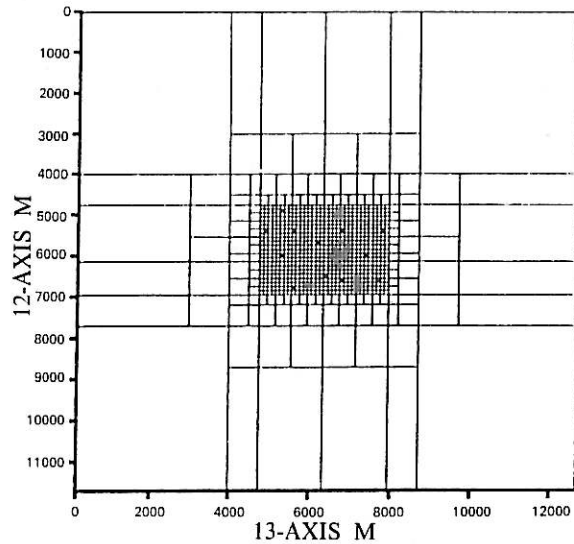


FIG. 16. Field scale miscible gas drive. Refined and gathered grid.

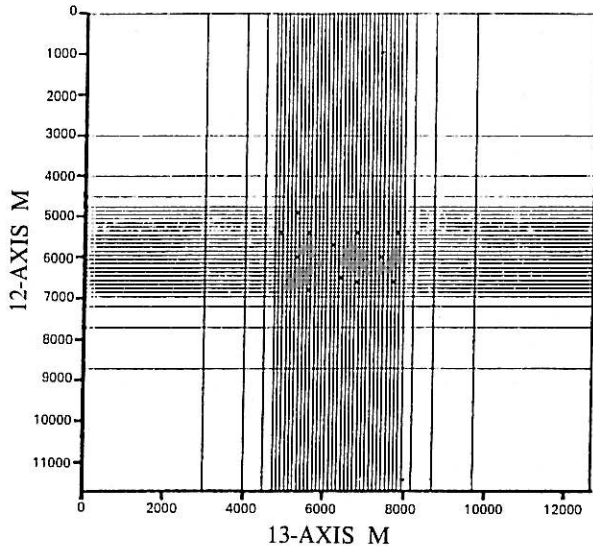


FIG. 17. Field scale miscible gas drive. The conventional Cartesian grid.

A 4×4 dynamic grid refinement was used on the edge of the miscible front. A 50×50 m block was refined if the gas saturation difference between the two upstream partial blocks (in the already 4×4 refined 50×50 m block), exceeded 0.2. The dynamic refined blocks were gathered if in the initially 50×50 m block the maximum saturation difference

between any partial blocks became less than 0.05. Fig. 18 shows the resulting block system after 3 years of injection. The actual block number is at this time 6640. A static conventional grid with the same block size in the EOR area requires 49,608 blocks already beyond the technical limit of compositional simulation. In Fig. 19 only the refined area is plotted showing more detail of it.

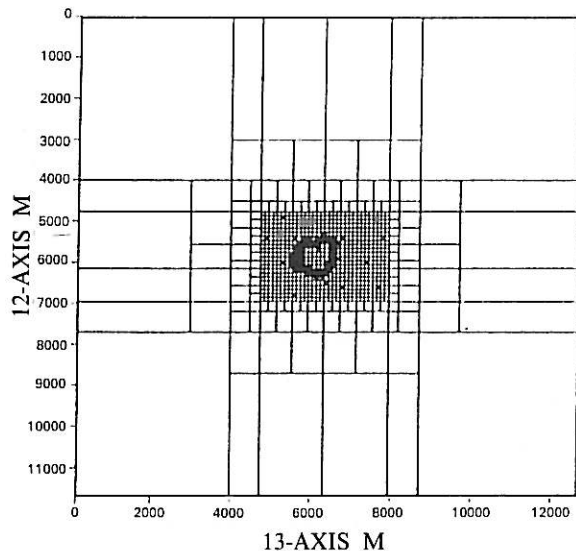


FIG. 18. Field scale miscible gas drive dynamic grid refinement after 3 years production.

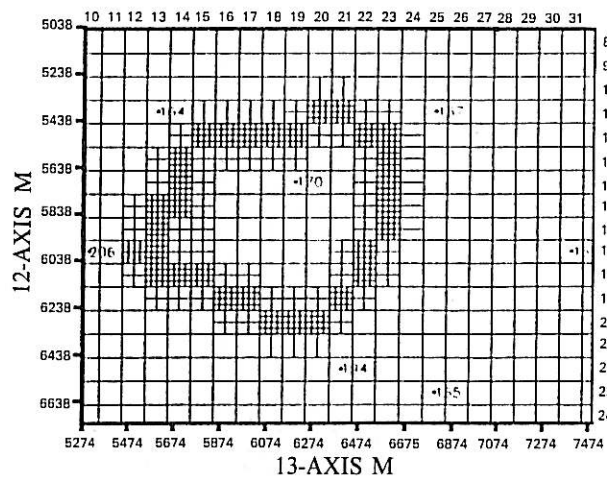


FIG. 19. Field scale miscible gas drive. Dynamic grid refinement after 3 years production focused on the EOR area.

CONCLUSIONS

1. Numerical simulation of EOR processes based on finite difference methods requires small block size. Depending on the displacement process the range is somewhere between 0.5 and 10 m. In full scale simulation, this is not applicable with conventional gridding for such a model would have some millions of grid blocks.

2. The grid must be orthogonal to make sure that the numerical solution converges to the true one if the grid size diminishes. By applying some simple rules, local grid refinement satisfies this requirement even at the fine-coarse grid transition zone for a Cartesian grid.
3. True refinement is robust and generally applicable, but requires new numerical algorithm and computer codes. Batch refinement can be adapted to conventional simulators, but its applicability is limited.
4. Small block size is only required at the displacing front. A dynamic grid refinement makes it possible to divide the downstream blocks ahead of the front and gather them in the upstream area.
5. The block gathering technique can be used outside the EOR area, reducing the block model to a two dimensional one. In this way, the influence of the environment (aquifer, other producing areas) is taken into account without wasting computing time for uninteresting detail.
6. Combining block gathering and dynamic grid refinement techniques an EOR displacement can be simulated with some meter block size on the front without exceeding the technical and economic limits.

NOMENCLATURE

A	surface of control volume in balance equation
A_{IJ}	surface common to grid blocks I and J
\vec{g}	gravity acceleration
h	grid spacing
K	number of all components
\bar{k}	permeability tensor
k_{ij}	component of the permeability tensor
k_{rp}	relative permeability for phase p
M_k	mole mass of component k
NJ	number of neighbours communicating with gridblock J
\vec{n}	unity normal vector on surface A
P	number of all phases
$P_{cpp'}$	capillary pressure for phase p and p'
p_p	phase pressure
Q_{IJ}	flow terms defined in Eq. 7
S_p	phase saturation
t	time
\vec{u}_p, u_p	filtration velocity of phase p
V	volume
x_{pk}	mole fraction, component k , phase p

Greek letters

Λ_{pk}	$\xi_p x_{pk} \lambda_p$
λ_p	phase mobility
ξ_p	specific mole density of phase p
ρ_p	phase density

τ_{IJ} interblock transmissibility
 ϕ porosity

Subscripts

p phase
 k component
 rp relative permeability for phase p
 I, J gridblocks

REFERENCES

- [1] Nghiem, L., 1983, An Integral Approach to Discretizing the Reservoir Flow Equations, CMG technical report.
- [2] Pedrosa, O.A. and Aziz, K., 1985, Use of Hybrid Grid in Reservoir Simulation, paper SPE 13507 presented at the Middle East Technical Conference, Bahrain.
- [3] Peaceman, D.W., 1977, Fundamentals of Numerical Reservoir Simulation. Development in Petroleum Science 6. Elsevier, Amsterdam, Oxford, New York.
- [4] Russel, T.F. and Wheeler, M.F., 1983, The Mathematics of Reservoir Simulation, Chapter II: Finite Element and Finite Difference Methods for Continuous Flows in Porous Media, Society for Industrial and Applied Mathematics, Philadelphia.
- [5] Ewing, R.E., 1983, The Mathematics of Reservoir Simulation, Chapter I: Problem Arising in the Modelling of Processes for Hydrocarbon Recovery of Processes for Hydrocarbon Recovery, Society for Industrial and Applied Mathematics, Philadelphia.
- [6] Perry, J.H. and Herron, E.H. Jr., 1969, Three-Phase Reservoir Simulation, J. Pet. Eng., pp. 211-210.
- [7] Snyder, L.J., 1969, Two-Phase Reservoir Flow Calculations, Soc. Pet. Eng. J., pp. 170-182.
- [8] Coats, K.H., 1980. An Equation of State Compositional Model, Soc. Pet. Eng. J., pp. 171-184.
- [9] Nghiem, L.X. and Li, Y.K., 1986, Effect of Phase Behavior on CO₂ Displacement Efficiency at Low Temperatures: Model Studies with an Equation of State, SPE Res. Eng., pp. 414-422.
- [10] Chu, C., 1981, The Course of Grid Size, AOS-TRA: Workshop on Computer Modelling.
- [11] Rian, D.T., 1988, Modelling and Simulation of Fluvial Geological System by Application of Front Tracking Methods, Case Study presented on the First International Forum on Reservoir Simulation, Alpbach.
- [12] Rosenberg von, D.U., 1982, Local Grid Refinement for Finite Difference Methods, paper SPE 10974 presented at the 57th Annual Fall Technical Conference, New Orleans.
- [13] Heinemann, Z.E., Gerken, G. and Meister, S., 1983, Anwendung der Localen Netzverfeinerung bei Lagerstaettensimulation, Erdoel und Erdgas, pp. 199-204.
- [14] Heinemann, Z.E., Gerken, G., Hantelmann, G., 1983, Using Grid Refinement in a Multiple-Application Reservoir Simulator, paper SPE 12255, presented at the 7th Symposium on Reservoir Simulation, San Francisco.
- [15] Heinemann, Z.E. and Brand, C., 1989, Gridding Techniques I in Reservoir Simulation, Proceeding of First and Second International Forum on Reservoir Simulation, Alpbach.
- [16] Ewing, R.E. and Lazarov, R.D., 1988, Adaptive Local Grid Refinement, paper SPE 17806, presented at the Rocky Mountains Regional Meeting, Casper, WY.
- [17] Brand, C. and Heinemann, Z. E., 1989, A New Iterative Solution Technique for Reservoir Simulation Equations on Locally Refined Grids, paper SPE 18410, presented 1989 at the 10th Reservoir Simulation Symposium on Reservoir Simulation, Houston.
- [18] Heinemann, Z.E. and Munka, M., 1986, Reservoir Simulation with Block Gathering, paper SPE 15097, presented at the 56th SPE California Regional Meeting, Oakland, CA.
- [19] Odeh, A.S., 1981, Comparison of Solutions to a Three-Dimensional Black-Oil Reservoir Simulation Problem, J. Pet. Tech., pp. 13-25.